OUKA
Osaka University Knowledge Archive

Title	Brazability and Erosion by Molten Filler Alloy of Aluminum Base Plates with Intermetallic Compounds(Materials, Metallurgy & Weldability)
Author(s)	Okamoto, Ikuo; Takemoto, Tadashi; Uchikawa, Kei
Citation	Transactions of JWRI. 1983, 12(1), p. 57-64
Version Type	VoR
URL	https://doi.org/10.18910/8981
rights	
Note	

Osaka University Knowledge Archive : OUKA

https://ir.library.osaka-u.ac.jp/

Osaka University

Brazability and Erosion by Molten Filler Alloy of Aluminum Base Plates with Intermetallic Compounds†

Ikuo OKAMOTO*, Tadashi TAKEMOTO** and Kei UCHIKAWA***

Abstract

Brazability and erosion by molten Al-10%Si filler alloy have been studied using laboratory made binary aluminum base plates with intermetallic compounds. Base plates were made by single addition of iron, nickel and zirconium up to 1 ~ 2.2 wt%, which contained Al_3Fe, Al_3Ni, Al_3Zr and Al_2Zr respectively. Fillet formation and spreading tests were performed in a vacuum (2×10^{-5} torr) at 605 ~ 625°C. All binary aluminum alloys with additional elements more than 1% exhibited undesirable fillet formation, because of the poor wetting of intermetallic compounds with molten filler alloys.

Base plates with fine recrystallization grain size showed large erosion depth. As molten filler alloy preferably penetrated along grain boundaries, base plates with higher recrystallization temperature were believed to provide large erosion depth. The dissolution process of base plate with intermetallic compound into molten filler alloy was seemed to be completed within holding time of 1 min during spread test, after that the isothermal solidification proceeded.

KEY WORDS: (Aluminum alloys) (Brazing) (Brazability) (Erosion) (Intermetallics)

1. Introduction

Fluxless brazing of aluminum including vacuum brazing techniques has been rapidly developed in recent years. The processes have been widely employed in the production of automotive heat exchangers. The use of brazing sheet with Al-Si-Mg cladding is the prominent feature of aluminum vacuum brazing. Investigations have been performed to improve the brazability by addition of some elements to Al-Si-Mg filler alloys for vacuum brazing[1)-5)] and Al-Si filler alloys for fluxless protective atmosphere brazing[6)]. Metallurgical factors influencing the brazability are composition[7)] and additional elements in filler alloys, grain size of α-Al[8)], silicon particle size[9)10)] and composition of base plates. Kawase *et al.*[11)] investigated the vacuum brazability of binary aluminum alloys with 0.1 ~ 3 wt% additional elements using Al-10%Si-1.5%Mg cladding and filler alloys. The results indicated that spreadability, flowability and ability of clearance filling were dependent on the vapour pressure of additional elements, melting point of base material and formation of intermetallic compounds.

In the brazing process of thin plates, the dissolution and erosion of base plate by molten filler alloy must be taken into consideration in relations to the brazing temperature and time, however, the effect of microstructure of base plate on the erosion of base plate has not been investigated precisely. The aim of this article is to investigate the reaction between molten Al-Si filler alloy and aluminum base plate with intermetallic compounds by the single addition of iron, nickel and zirconium.

2. Experimental Procedures

Binary aluminum alloys were made from 99.99% aluminum and high purity Al-X (X: additional elements) mother alloys. The alloys were melted in a vacuum and cast into molds of 15 x 15 x 40 mm and then homogenized, hot rolled, intermediate annealed and finally cold rolled to the plates of 3 mm thickness with 80% reduction. **Table 1** shows the chemical compositions of base plates. All alloys except Al-Si alloys have intermetallic compounds. Al-Si alloys were used for the comparison with the plates with intermetallic compounds.

† Received on April 30, 1983
* Professor
** Research Instructor
*** Graduate School, Osaka University (Present address: Ajikawa Iron Works & Construction Co., Ltd., Osaka)

Transactions of JWRI is published by Welding Research Institute of Osaka University, Ibaraki, Osaka 567, Japan

Table 1 Chemical composition of base plates (wt%)

Alloy	Element	Alloy	Element
M-1	0.00Fe	Z-1	0.06Zr
M-2	0.15Fe	Z-2	0.23Zr
M-3	0.51Fe	Z-3	0.5 Zr*
M-4	1.20Fe	Z-4	1 Zr*
M-5	2.00Fe	1100	**
S-1	0.14Si	N-1	0.5Ni
S-3	0.32Si	N-2	1 Ni*
S-3	0.84Si	N-3	2 Ni*

Other impurities: 0.001 ~ 0.009

* : Nominal composition

** 1100 : 0.23Fe, 0.08Si, 0.03Cu, 0.02Mn, others < 0.01

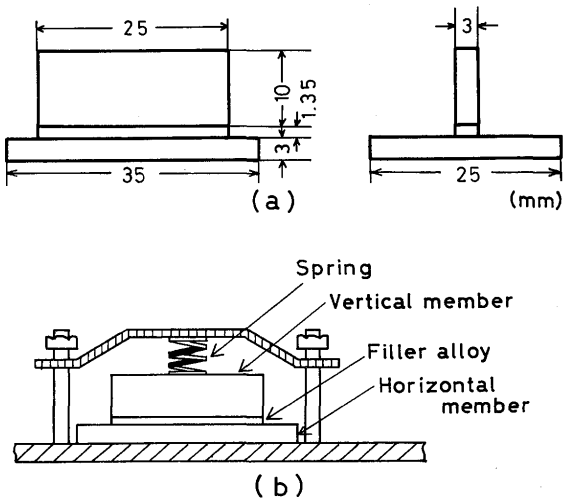

Fig. 1 Shape and size of braze specimen

Figure 1 (a) shows the shape and size of braze specimen. The rolling direction is parallel to longitudinal direction of horizontal base plate and normal to that of vertical one. Filler alloy ($25^l \times 3^w \times 1.35^t$) was preset between vertical and horizontal plates and a load of 20 g/mm^2 was applied to the filler alloy by pushing a vertical plate with a heat resistant spring (Fig. 1 (b)). The filler alloy is **BA 4045** alloy with the composition of Al-9.73%Si-0.13%Fe. Prior to brazing, both base plates were abraded by 600 grade emery paper and degreased in an ultrasonic aceton bath. Brazed specimens were cut at center and polished for the measurement of fillet leg length. The fillet leg length ratio, L_V/L_H (L_V ; vertical leg length, L_H : horizontal leg length), was used for the evaluation of brazability. Brazing results is considered to be preferable as the value approached 1[10)12)].

Spread test was employed to investigate the reaction between base plate and molten filler alloy. Filler alloy (2 x 2 x 0.5, mm) was put at the center of electropolished base plate (25 x 25 x 3, mm) and a load of 20 g/mm^2 was applied on the filler alloy. They were heated to test temperature up to 625°C and held for certain times less than 30 min. After microscopic observation on the spread front, specimens were cut at the center of specimen and the erosion depth of base plate by molten filler alloy was measured by a profile projector. Brazing and spread tests were performed under the vacuum level of 2 x 10^{-5} torr. The structure of intermetallic compounds were analized by X-ray diffraction (diffractometer, CuKα , 35 kV, 10 mA).

3. Experimental Results

3.1 Brazability of aluminum alloys with intermetallic compounds

The additional elements of Fe, Zr and Ni forms intermetallic compounds with aluminum. Micrograghs of Al-Fe and Al-Ni base plates are shown in **Fig. 2** and **3** respectively. The compounds distributed along the rolling direction, and the amount increased with the content of additives, the size of compounds was not so changed in Al-Fe alloys but the size was increased in Al-2%Ni base plate. The other base plates with Zr had also intermetallic compounds and its amount increased with the content of additional elements. **Tables 2** and **3** indicate the results of X-ray diffraction analysis on base plates with iron and nickel respectively. It is noted that each base alloy has intermetallic compounds of Al_3Fe and Al_3Ni, respectively. The diffraction lines corresponding to Al_3Zr and Al_2Zr were observed in Al-Zr alloys. Pure aluminum base plate (M-1, 00.001%Fe), of course, showed no compounds.

The effects of content of additional elements on the fillet leg length ratio (L_V/L_H) of the specimens brazed at 605°C for 3 min are represented in **Fig. 4**. The values are relatively high in M-1 pure aluminum plate, but the addition of Ni and Si drastically decreases them with the increase in content. The addition of Zr and Fe scarsely influenced on L_V/L_H up to 0.5%, but the values became less than 0.7 as the content exceeded 1%. Sound fillet form could not be achieved in Al-2%Fe and Al-2%Ni base plate under brazing temperature of 605°C. The fillet did not exhibit concave surface showing that the unsatisfactory brazability was attributed to the poor wettability of base plates.

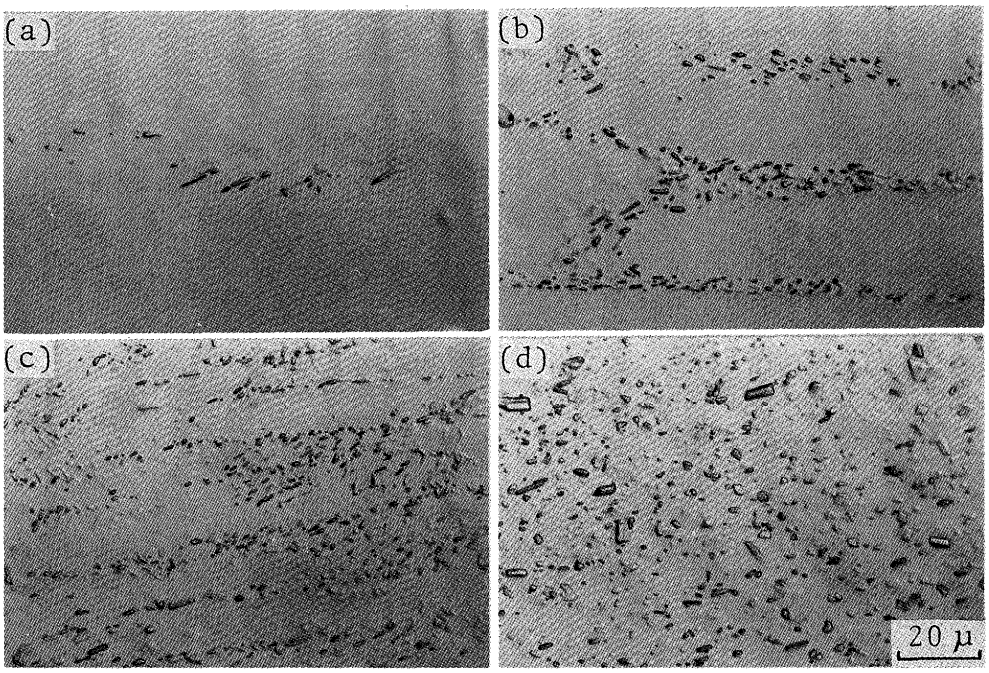

Fig. 2 Micrographs of base plates containing iron, (a) M-2 (0.15%Fe), (b) M-3 (0.51%Fe), (c) M-4 (1.2%Fe) and (d) M-5 (2.0%Fe)

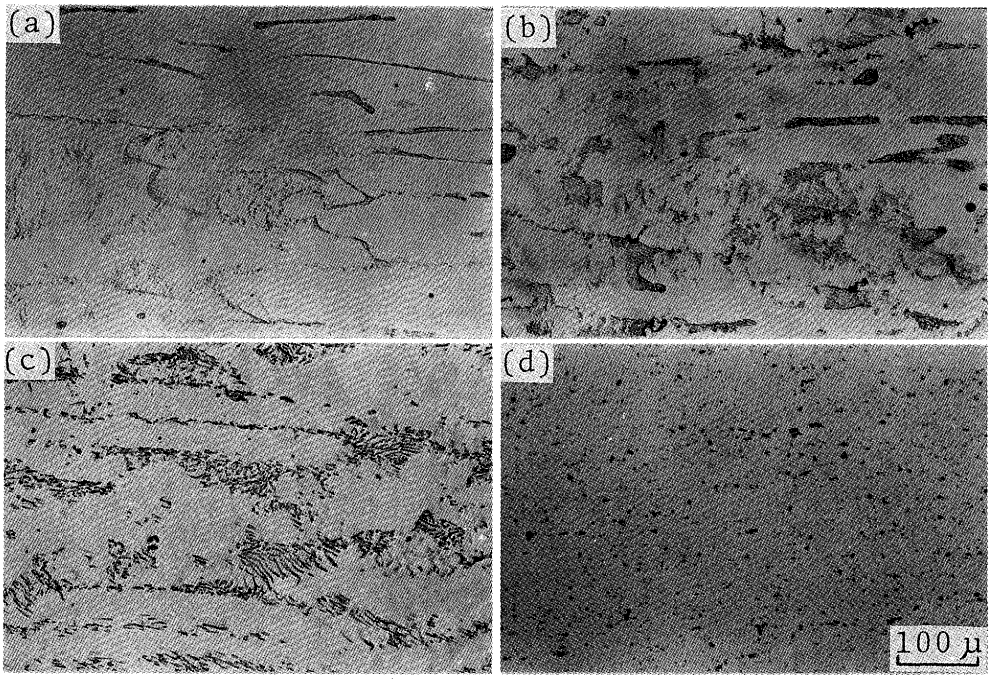

Fig. 3 Micrographs of base plates containing nickel, (a) N-1 (0.5%Ni), (b) N-2 (1%Ni), (c) N-3 (2%Ni) and **1100** commercial alloy (d)

Figure 5 shows the micrographs of spread front of base alloys with iron. Smooth spread front is shown in pure base metal, but intricated morphology becomes remarkable with the increase in iron content. The tendency was similar in the other base plates with Zr and Ni. **Figure 6** is the spread front indicating the molten alloy flew along recrystallized grain boundary. **Figure 7** shows the effect of the content of additional elements in base plates (at%) on recrystallized grain size of base plate. The grain size decreased with the increase in the content of additional elements. On the other hand, microscopic observations revealed that intermetallic compounds acted as

Table 2 X-ray diffraction analysis of Al-Fe system base plates

Observations				ASTM data			
1100		M-5 (Al-2%Fe)		Al		Al_3Fe	
d (Å)	I	d (Å)	I	d (Å)	I/I_o(%)	d (Å)	I/I_o(%)
2.344	VS	2.344	VS	2.338	100	2.34	40
		2.265	vw			2.25	40
						2.23	40
						2.12	40
2.099	vw	2.103	W			2.09	100
		2.085	vw			2.08	40
		2.062	vw			2.06	40
						2.04	100
2.027	VS	2.027	VS	2.024	47	2.02	100
		1.989	vw			1.98	20
		1.941	W			1.93	40
						1.91	20
		1.478	vw			1.45	60
1.433	M	1.433	S	1.431	22	1.43	60
						1.41	20
						1.40	40
						1.37	20
1.354	vw	1.354	vw			1.35	40
1.295	vw	1.293	vw			1.29	60
		1.290	vw			1.28	20
1.221	VS	1.222	S	1.221	24		
1.170	S	1.170	M	1.169	7	$(I/I_o \geq 20)$	

Intensity VS > S > M > W > vw

Table 3 X-ray diffraction analysis of Al-2%Ni base plate

observation		ASTM data			
N-3 (Al-2%Ni)		Al		Al_3Ni	
d (Å)	I	d (Å)	I/I_o(%)	d (Å)	I/I_o(%)
3.440	vw			3.44	100
3.018	vw			3.01	60
				2.71	3
2,592	vw				
2.550	vw			2.55	30
2.468	vw			2.46	40
2.404	W			2.40	20
2.338	VS	2.338	100		
				2.26	5
2.186	vw			2.18	70
2.161	W			2.16	80
2.067	vw			2.07	100
2.023	VS	2.024	47	2.01	40
				2.00	90
1.969	vw			1.97	70
1.929	vw			1.93	100
1.881	vw			1.88	30
				1.84	30
				1.76	20
1.433	S	1.431	22		
1.222	VS	1.221	24		
1.170	W	1.169	7		

Intensity VS > S ≫ W > vw

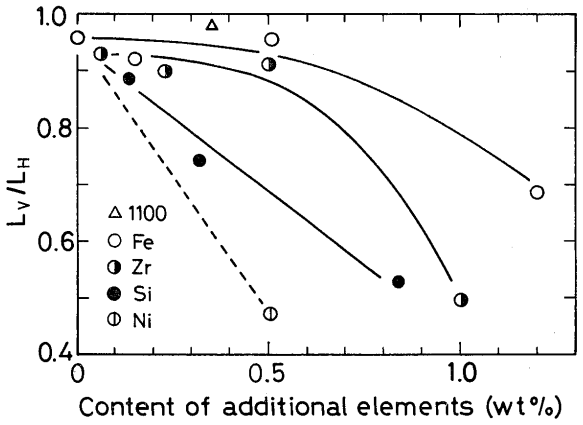

Fig. 4 Relations between content of each additional element

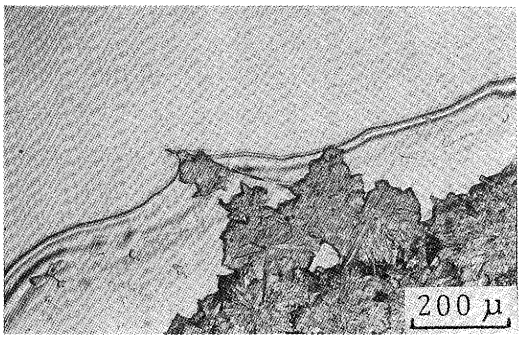

Fig. 6 Spreading of filler alloy grain boundary of base plate surface

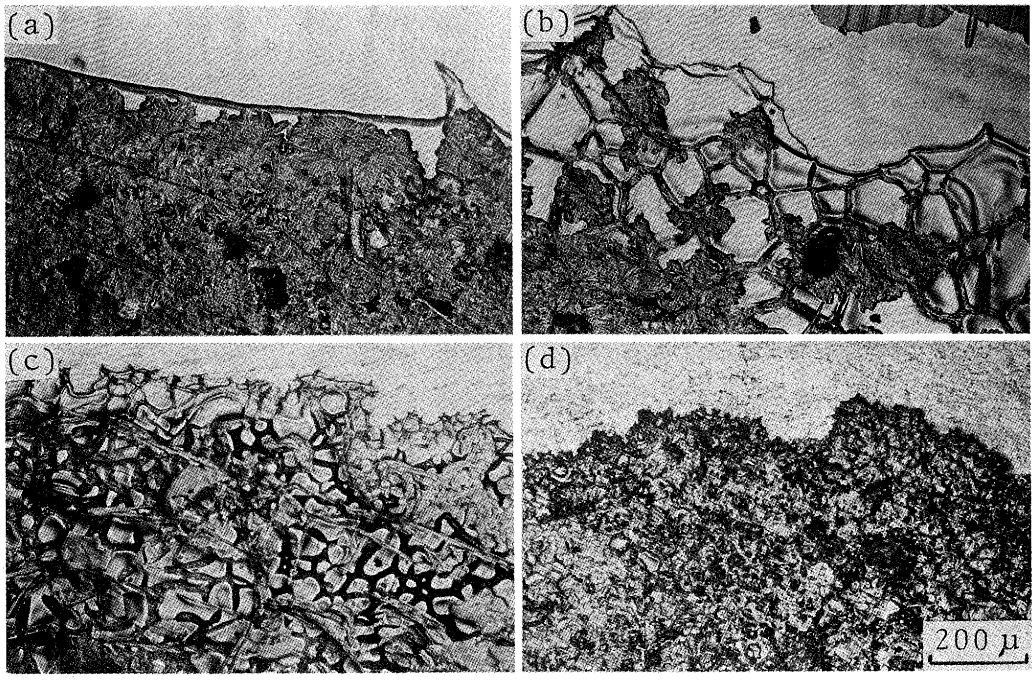

Fig. 5 Micrographs of spread front of base plate with various iron content, (a) M-1 (0%Fe), (b) M-2 (0.15%Fe), (c) M-3 (0.51%Fe) and (d) M-5 (2.0%Fe)

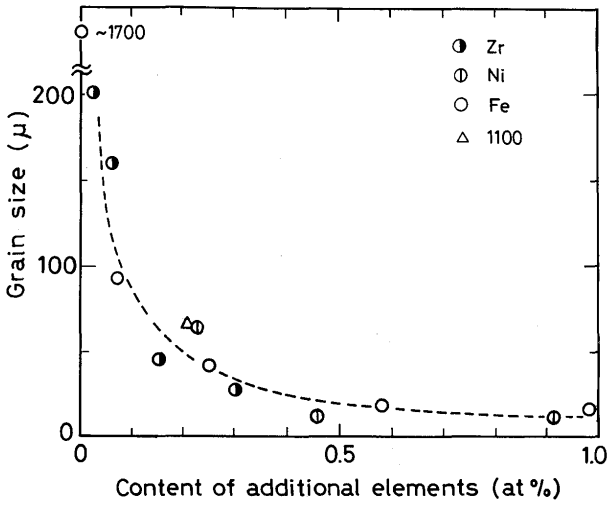

Fig. 7 Effect of content of additional elements in base plate on recrystallized grain size of base plate

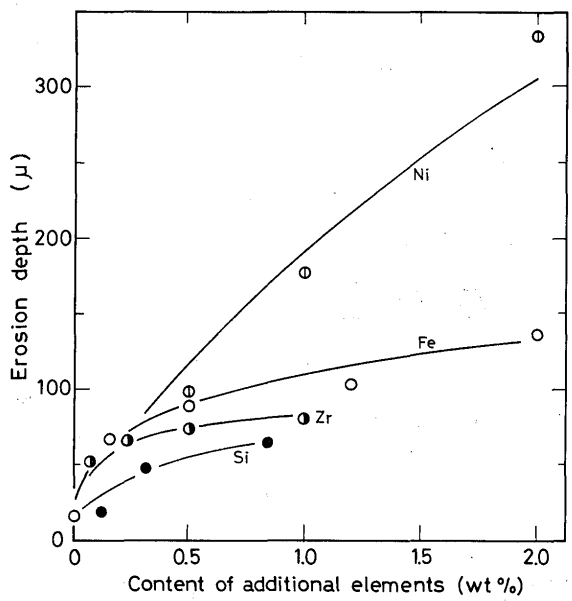

Fig. 8 Effect of content of additional elements on erosion depth after spread test at 615°C for 3 min

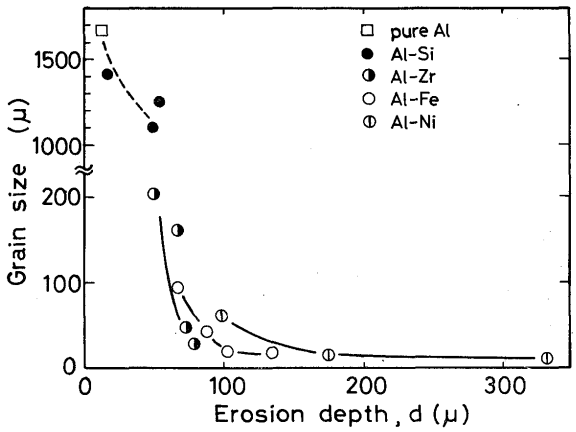

Fig. 9 Relation between recrystallized grain size of aluminum plate and erosion depth after spread test at 615°C for 3 min

obstacles against the flow of molten filler alloy. Consequently, it is concluded that the cause of intricated spread front with the increase of additional elements resulted in the decrease in recrystallized grain size and the increase in the amount of intermetallic compounds.

3.2 Erosion of base plate by molten filler alloy

Figure 8 indicates the effect of the content of additional elements on the erosion depth of base plate after spread test at 615°C for 3 min. The depth increased with the content of additional elements. When comparing the erosion depth at the same content of additional elements (wt%), the depth increased in this order: Si, Zr, Fe and Ni. **Figure 9** demonstrates the relations between recrystallized grain size after 615°C spread test for 3 min and erosion depth. The depth became large with the decrease in grain size, however, the depth was not remarkably influenced by grain size less than 30 μ, indicating that the other factors strongly influenced the erosion reaction. Similar to the morphology of spread front, the erosion depth was influenced by the amount of intermetallic compounds in base plate because the depth became large with the increase in content of additional elements which corresponded the amount of intermetallic compounds. Accordingly, the interface between intermetallic compounds and matrix is also considerable to the path of erosion of base plate in addition to the recrystallized α-Al grain boundary. When comparing the erosion depth at the same grain size, it increased in the following order of additional elements: Zr, Fe and Ni.

Figure 10 shows the relations between the erosion depth and holding time at 605 ~ 625°C during spread tests of M-1 and M-4 base plates. In every test conditions, erosion depths of M-4 base plate are larger than those of M-1 base plate, indicating that the former is easy to be eroded by molten filler alloy. The plots of erosion depth (d) and the square root of holding time (t) showed linear relationships. Therefore, the relation between d and t is represented as $d = k\sqrt{Dt}$ (D: diffusion coefficient, cm^2/sec, k: constant). From the inclination of the plots of d-$\sqrt{t}$, $k\sqrt{D}$ is determined at each temperature. The Arrenius type plots of $k\sqrt{D}$ vs $1/T$ (T: temperature, K) are shown in **Fig. 11.** The temperature dependence of D is appreciably larger than that of the impurity diffusion coefficient in aluminum under the hypothesis that k is a constant. Consequently, the apparent activation energies

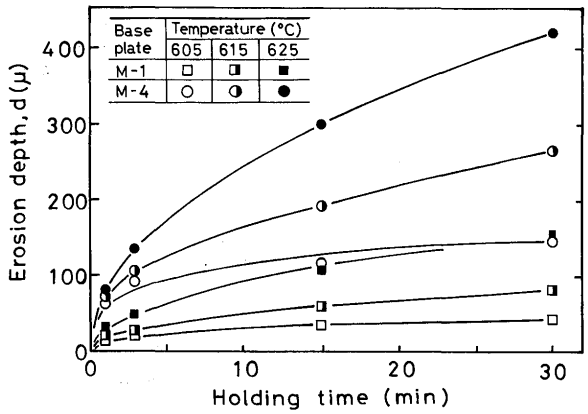

Fig. 10 Changes of erosion depth of base plate M-1 and M-4 during heating at 605 ~ 625°C

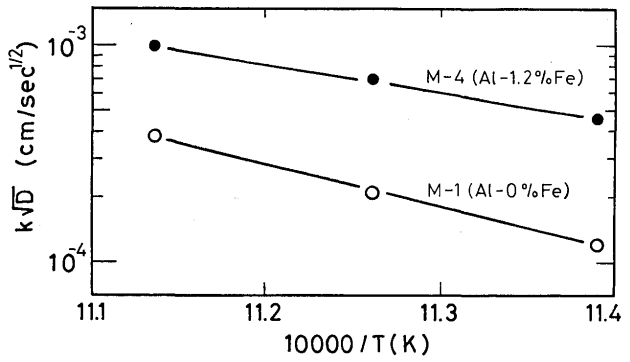

Fig. 11 Plots of $k\sqrt{D}$ vs. $1/T$

calculated from the slope of Fig. 11 were 180 and 121 kcal/mol for M-1 and M-4 base plates respectively. When comparing the obtained values with the activation energy for the diffusion of Si in aluminum (29.6 ~ 32.5 kcal/mol), the obtained values are remarkably large. The difference can be interpreted by the following factors: the reaction was proceeded under interfacial rate control, k had the temperature dependence and the amount of used filler alloy was extremely small.

Figure 12 demonstrates the schematic illustration of erosion area for the calculation of the volume of erosion area and mean Si concentration in erosion area. The volume of erosion area (V_e) is represented by the following equation, $V_e = (Rd^2 - d^3/3)$, under the hypothesis that the area is a part of the sphere with radius of R ($R = (4d^2 + W^2)/8d$, where, d: erosion depth, w: width of erosion area). Consequently the sum of the volume of erosion area and used filler alloy, V, is represented by the following equation, $V = V_e + V_o = \pi(Rd^2 - d^3/3) + V_o$, where, V_o: volume of used filler alloy. The value of V is obtained by the microscopic observation data of d and W, therefore, the mean Si concentration in hatched area and

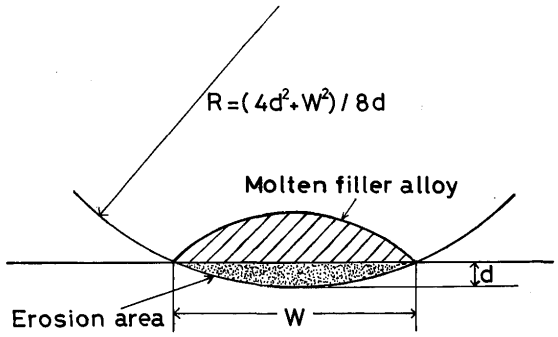

Fig. 12 Schematic illustration of erosion area for the calculation of the volume of erosion zone

Table 4 Calculated mean Si content of erosion zone in M-1 and M-4 base plate after spread test for 3 min and 1 min respectively

Test temperature (°C)	Mean Si content (wt%)		Si concentration of liquidus (wt%)
	M-1 (0%Fe) 3 min	M-4 (1.2%Fe) 1 min	
605	9	8.5	8
615	7	7	6.5
625	5	5	5

erosion area in Fig. 12 is calculated by neglecting the changes of density before and after reaction.

$$[\text{mean Si concentration, wt\%}] = 9.73 V_o/V$$

The value of 9.73 is the Si content of used filler alloy. The calculated results are indicated in **Table 4** for M-1 and M-4 base plates brazed at 605 ~ 625°C for 3 and 1 min respectively. The calculated mean Si concentration was nearly equal to the Si concentration of molten liquid at each temperature. Mean Si concentration was lowered by further holding. As the composition of liquid is maintained constant at each holding temperature, solid α-Al crystallizes by further holding time. This means that the dissolution reaction of aluminum base plate is terminated at the time shown in Table 4, 3 min for M-1 base plate and 1 min for M-4 base plate. In the prolonged brazing, the process changes into the isothermal solidification process crystallizing the α-Al according to the diffusion of Si into base plate.

4. Discussions

The all additional elements lowered the brazability evaluated by the fillet form. After Kawase *et al.*[11], the single addition of Fe, Mn, Cr and Ti reduced the spreadability and flow factor with the increase in the additional amount, however, the elements showed no influence on

the filled clearance length. The evaluating parameter L_V / L_H would be corresponded to the filled clearance length because those parameters are based on the ability of fillet formation. In the present work, however, L_V / L_H was decreased with the increase of the intermetallic compounds in base plate. The difference seems to depend on the Mg content of filler alloys. Kawase *et al.*[11], used Mg bearing filler alloy, however, the alloy without Mg was used in this work. As the filler alloy without Mg has no gettering reaction, the surface properties of intermetallic compounds strongly affect the wetting and the other brazing characteristics. On the other hand, the filler alloy with Mg compenstates the hindrance effect of compound against wetting by the gettering action of Mg[13]. The grain boundary is shown to be the preferential flowing path of molten filler alloy in Fig. 6. As the base material with intermetallic compounds has fine recrystallized grain size, the material is thought to exhibit large spread area, however, the spread area was not dependent on the amount of intermetallic compounds and grain size. This seems to be caused by the hindrance effect of intermetallic compounds against the wetting of molten filler alloy, because the solubility of intermetallic compounds in filler alloy seems to be very small and it has been noted that solubility of some extent is necessary to spread[14]. Therefore the difference in the degree of decrease of L_V / L_H by each additional elements is seemed to depend on the difference in solubility which is necessary to spread[14] and moreover the properties of the surface oxide films on the intermetallic compounds[11].

Kawase *et al.*[11], investigated the effect of additional elements on the erosion depth of binary aluminum base plate. Form the results, it is shown that the erosion depth of base plates with 1.3 at% additional elements was increased in the following ascending order: Mn<Ti<Cr<Fe. In the present work, when comparing at about 0.5 at% (0.3 at% in Al-Zr base plate), the erosion depth of base plate increased in this order: Zr≦Fe<Ni. On the other hand, the recrystallization temperature of binary aluminum increased the following order of additional elements[15]; Ti≦Mn<Cr<Zr<Fe. When rapidly heated to brazing temperature, the rate of recovery and recrystallization of base plate with higher recrystallization temperature is relatively slower than that of low recrystallization temperature base plate. Consequently, the cold work structure is maintained for longer times in the former base plates. As a result, the base plate with higher recrystallization temperature has higher defect density and provides the easy path for dissolution of base plate and diffusion of Si. In fact, the erosion depth of recrystallized **1100** aluminum after annealing at 610°C for 1 hr was reduced to about 70% of that of the cold rolled plate. There appears to be good correlation between the erosion depth of binary aluminum base plate and the recrystallization temperature, *i.e.*, from the work after Kawase *et al.*[11] and the present results, it can be said that the erosion depth increased with increasing the recrystallization temperature of aluminum base plate. On the other hand, the effect of additional elements, which forms solid solution but not intermetallic compounds, on erosion depth was revealed to increase in the following order[11]: Mg ≒ Zn<Cu<Si. The recrystallization temperature of these alloys are ranging about 200°C[16] but slightly increased in this order; Cu ≒ Zn<Mg ≒ Si, therefore, there is no good correlation between the recrystallization temperature and the erosion depth. The base plates containing Si has large recrystallization grain size as shown in Fig. 9, however, the erosion depth of base plate with relatively large amount of Si is nearly equal to that of the small addition of Zr. Consequently the properties of alloying element itself seems to influenced the erosion reaction especially in the base plate with relatively large amount of additional elements. As mentioned above, the erosion of aluminum base plate is influenced by kind and the amount of soluble elements in solid solution, the use of the base plate having same grain size and extremely small amount of elements within solubility is suggested to be an excellent procedure to clear precisely the erosion phenomena of aluminum base plate by molten filler alloy.

5. Conclusions

The brazability and erosion by molten filler alloy of aluminum base plate with intermetallic compounds were investigated using Al-10%Si filler alloy. The obtained results are summarized as follows.

(1) The brazability evaluated by the fillet leg length ratio (L_V / L_H) was reduced as the amount of elements, which formed intermetallic compounds, in base plate increased. The reason was thought to be attributable to the difficulty of wetting between intermetallic compounds and molten filler alloy due to the small solubility between them.

(2) The erosion depth of base plate by molten filler alloy was increased with the decrease in the recrystallized grain size of base plate. The erosion depth was seemed to be relatively large in the base plate with higher recrystallization temperature.

(3) The dissolution reaction of base plate with intermetallic compounds during spread tests on the base plate was thought to be completed within 1 min at 605 ~ 625°C, and it was indicated that the isothermal solidification proceeded beyond this holding time.

(4) The morphology of spread front of pure aluminum

base plate was smooth, on the other hand, the morphology became irregular with increasing the amount of intermetallic compounds. The irregularity of spread front in base plates was thought to attributed that the compounds acted as obstacles against the flow of molten filler alloy on base plate and the fine recrystallized grain size as the molten filler alloy preferentially flows along the recrystallized grain boundaries.

Acknowledgement

The authors would like to thank Dr. Yoshihiko Sugiyama and Mr. Hiroshi Irie at Sumitomo Light Metal Industries Ltd. for chemical analysis. Thanks are also to Dr. Minoru Yokota at Sumitomo Electric Industries Ltd. for preparing the Al-Fe mother alloys.

References

1) H. Kawase, M. Yamaguchi: J. Light Metal Weld. & Construction **15**(1977), No. 8, 345 (in Japanese).

2) U.S.P.: 3,898,053; 3,963,453; 3,963,454.

3) S. Imaizumi: J. Light Metal Weld. & Construction, **14**(1976), No. 2, 569 (in Japanese).

4) H. Yoshida, Y. Takeuchi: J. Japan Inst. Light Metals, **27** (1977), No. 3, 122 (in Japanese).

5) Patent: S 53-55443 (Japan).

6) H. Schöer, W. Schultze: Z. Metallkde., **63**(1972), 775., Patent: S 50-4466 (Japan).

7) H. Kawase, M. Yamagichi, K. Tanaka: J. Light Metal Weld. & Construction, **11**(1973), No. 3, 115 (in Japanese).

8) P. Sharples: Weld. J., **54**(1975), No. 3, 164.

9) R. A. Woods; Aluminum, **54**(1978), 444.

10) I. Okamoto, T. Takemoto: J. Japan Inst. Light Metals, **31** (1981), No. 8, 539 (in Japanese).

11) H. Kawase, M. Yamaguchi: J. Light Metal Weld. & Construction, **16**(1978), No. 4, 159 (in Japanese).

12) I. Okamoto, T. Takemoto: J. Japan Weld. Soc., **37**(1978), No. 12, 816 (in Japanese).

13) J. R. Terill, C. N. Cochran, J. J. Stokes and W. E. Haupin: Weld. J., **50**(1971), No. 12, 833.

14) V. R. Miller and A. E. Schwaneke: Weld. J., **57**(1978), No. 10, 303-s.

15) K. Ogawa, S. Inoue, T. Kobayashi: The Furukawa Electric Review, No. 66 (1979), 63 (in Japanese).

16) K. Hirano; J. Japan Inst. Light Metals, **31**(1981), 206 (in Japanese).